

## An exhaustive theoretical analysis of thermal effect inside bubbles for weakly nonlinear pressure waves in bubbly liquids

Cite as: Phys. Fluids **33**, 053302 (2021); <https://doi.org/10.1063/5.0028655>

Submitted: 07 September 2020 . Accepted: 10 December 2020 . Published Online: 04 May 2021

 Takafumi Kamei (亀井陸史),  Tetsuya Kanagawa (金川哲也), and  Takahiro Ayukai (鮎貝崇広)



View Online



Export Citation



CrossMark

**Physics of Fluids**

**SPECIAL TOPIC:** Tribute to  
Frank M. White on his 88th Anniversary

SUBMIT TODAY!



# An exhaustive theoretical analysis of thermal effect inside bubbles for weakly nonlinear pressure waves in bubbly liquids

Cite as: Phys. Fluids **33**, 053302 (2021); doi: 10.1063/5.0028655

Submitted: 7 September 2020 · Accepted: 10 December 2020 ·

Published Online: 4 May 2021



View Online



Export Citation



CrossMark

Takafumi Kamei (亀井陸史),<sup>1</sup> Tetsuya Kanagawa (金川哲也),<sup>2,a)</sup> and Takahiro Ayukai (鮎貝崇広)<sup>1</sup>

## AFFILIATIONS

<sup>1</sup>Department of Engineering Mechanics and Energy, Graduate School of Systems and Information Engineering, University of Tsukuba, 1-1-1 Tennodai, Tsukuba 305-8573, Japan

<sup>2</sup>Department of Engineering Mechanics and Energy, Faculty of Engineering, Information and Systems, University of Tsukuba, 1-1-1 Tennodai, Tsukuba 305-8573, Japan

<sup>a)</sup>Author to whom correspondence should be addressed: [kanagawa.tetsuya.fu@u.tsukuba.ac.jp](mailto:kanagawa.tetsuya.fu@u.tsukuba.ac.jp)

## ABSTRACT

Weakly nonlinear propagation of pressure waves in initially quiescent compressible liquids uniformly containing many spherical microbubbles is theoretically studied based on the derivation of the Korteweg–de Vries–Burgers (KdVB) equation. In particular, the energy equation at the bubble–liquid interface [Prosperetti, J. Fluid Mech. **222**, 587 (1991)] and the effective polytropic exponent are introduced into our model [Kanagawa *et al.*, J. Fluid Sci. Technol. **6**, 838 (2011)] to clarify the influence of thermal effect inside the bubbles on wave dissipation. Thermal conduction is investigated in detail using some temperature-gradient models. The main results are summarized as follows: (i) Two types of dissipation terms appeared; one was a well-known second-order derivative comprising the effect of viscosity and liquid compressibility (acoustic radiation) and the other was a newly discovered term without differentiation comprising the effect of thermal conduction. (ii) The coefficients of the KdVB equation depended more on the initial bubble radius rather than on the initial void fraction. (iii) The thermal effect contributed to not only the dissipation effect but also to the nonlinear effect, and nonlinearity increased compared with that observed by Kanagawa *et al.* (2011). (iv) There were no significant differences among the four temperature-gradient models for milliscale bubbles. However, thermal dissipation increased in the four models for microscale bubbles. (v) The thermal dissipation effect observed in this study was comparable with that in a KdVB equation derived by Prosperetti (1991), although the forms of dissipation terms describing the effect of thermal conduction differed. (vi) The thermal dissipation effect was significantly larger than the dissipation effect due to viscosity and compressibility.

© 2021 Author(s). All article content, except where otherwise noted, is licensed under a Creative Commons Attribution (CC BY) license (<http://creativecommons.org/licenses/by/4.0/>). <https://doi.org/10.1063/5.0028655>

## I. INTRODUCTION

The pressure wave in a liquid containing many spherical microbubbles develops into a shock wave owing to the competition between a wave nonlinearity and a dissipation of the medium or into a solitary wave through competition between the wave nonlinearity and a dispersion due to bubble oscillations.<sup>1,2</sup> As there are significant differences between shock and solitary waves, it is important to determine whether the pressure wave develops into the shock wave or the solitary wave. Therefore, quantitative understanding of the nonlinearity, dissipation, and dispersion of the pressure wave is desired. However, it is difficult to understand the

contributions of the nonlinearity, dissipation, and dispersion of the pressure wave to wave propagation directly through experiments or numerical simulations.<sup>3–9</sup> For weakly nonlinear pressure waves,<sup>10</sup> we can theoretically derive the weakly nonlinear wave equation as an approximate equation describing the spatio-temporal development of the waveform obtained owing to the balance among the nonlinearity, dissipation, and dispersion of the wave.<sup>10</sup> Then, we can understand the relative sizes of the dissipation and dispersion contributing to the nonlinearity. There are many types of weakly nonlinear wave equations describing nonlinear wave propagation in bubbly liquids.<sup>11–27</sup> In particular, the Korteweg–de Vries–Burgers

(KdVB) equation for a long wave with a low frequency is one of the most famous equations because it is derived in many theoretical studies;<sup>11–13,17,18,24–27</sup> moreover, its solution agrees with the waveforms observed in several experiments.<sup>28–30</sup>

van Wijngaarden<sup>2</sup> conducted pioneering work in deriving the Korteweg–de Vries (KdV) equation for pressure waves in a bubbly liquid but did not consider the dissipation effect. Subsequently, van Wijngaarden<sup>11</sup> derived the KdVB equation incorporating the dissipation effect. Following the derivation of the KdVB equation by van Wijngaarden,<sup>11</sup> several researchers derived the KdVB equations considering different scenarios involving bubbly liquids. In particular, Kuznetsov *et al.*<sup>28</sup> proved that the experimental results and theoretical predictions obtained using the KdVB equation incorporating viscosity, compressibility, and thermal conductivity of a bubbly liquid agreed well. Prosperetti<sup>13</sup> examined the effect of thermal conduction on single bubble oscillations, incorporated its result into basic equations for bubbly liquids, and then derived KdVB equations considering dissipation effects due to thermal conduction. The incorporation of compressibility and thermal conduction in deriving the KdVB equation by Kuznetsov *et al.*<sup>28</sup> may be empirical. Later, a detailed explanation on dissipation due to thermal conduction was provided by Prosperetti.<sup>13</sup> In this work,<sup>13</sup> in addition to the thermal conduction, the liquid viscosity at the bubble–liquid interface was considered, but liquid compressibility was not considered. Furthermore, although an effective polytropic exponent was introduced,<sup>13</sup> the effect of thermal conduction was discussed only in terms of isothermal or adiabatic processes. The influence of the effective polytropic exponent, which reflects the thermodynamic process inside the bubble, has not been investigated adequately. Recently, in our theoretical studies on waves in bubbly liquids,<sup>17,18</sup> the viscosity at the bubble–liquid interface and liquid compressibility as the dissipation effect were considered; moreover, the viscosity of the bubbly liquid and thermal conduction through the bubbly liquid were also considered.<sup>31,32</sup>

Table I summarizes the four dissipation factors used in the present and previous studies.<sup>13,18</sup> There is no exhaustive study incorporating these four dissipation factors on nonlinear wave propagation, except for the present study. Therefore, the purpose of this study is to derive the KdVB equation incorporating the four dissipation factors, i.e., the viscosity of the bubbly liquid and that at the bubble–liquid interface, thermal conduction at the bubble–liquid interface, and acoustic radiation due to liquid compressibility. Based on the derived KdVB equation, we focus on analyzing the thermal conduction at the interface and thermodynamics inside the bubble to theoretically clarify their effects on nonlinear wave propagation. We also utilize some popular models for evaluating the temperature-gradient

at the bubble–liquid interface using (11) and determine the differences among these models.

This paper is organized as follows: Section II introduces the basic equations and perturbation expansions based on the multiple-scales method.<sup>10</sup> In particular, the energy equation for the bubble–liquid interface and the effective polytropic exponent<sup>13</sup> are incorporated into our model to investigate the thermal effect. Section III presents the derivation of the KdVB equation and explains the appearance of two dissipation terms; one is the well-known second-order derivative with respect to the space and the other is a newly discovered term without differentiation. Section IV describes the coefficients of the KdVB equation and clarifies the difference among the present and previous coefficients. We observe that the thermal effect contributes not only to wave dissipation but also to wave nonlinearity, and thermal conduction strongly contributes to dissipation. Section V presents the conclusions of the study.

## II. PROBLEM FORMULATION

### A. Problem

We consider one-dimensional (i.e., plane) weakly nonlinear pressure waves with a low frequency and long wavelength in a liquid uniformly containing many spherical gas bubbles. We focus on examining the effect of the thermal conduction at the bubble–liquid interface on wave propagation.

We use the following assumptions for formulating the problem: (i) The bubbly liquid is initially quiescent. (ii) The bubbles do not coalesce, break up, appear, and disappear. (iii) The gas viscosity and bulk viscosity are ignored. (iv) The phase change and mass transport across the bubble–liquid interface are ignored. (v) The temperature of the liquid phase is constant. (vi) The effect of mass transfer<sup>33</sup> is neglected; we will extend the recent result of linear theory<sup>33</sup> to weakly nonlinear theory in our forthcoming study. (vii) The theory of dynamics of an encapsulated bubble (i.e., the effect of a shell of the bubble) has recently been established<sup>34,35</sup> for a medical application such as a contrast agent.<sup>36</sup> Although the effect of the shell is ignored in this study for simplicity, our another study investigated the effect of the elasticity and viscosity of the shell on each coefficient in the KdVB equation.<sup>37</sup>

### B. Basic equations

We use the following conservation equations of mass and momentum for bubbly liquids:<sup>38–40</sup>

$$\frac{\partial \rho^*}{\partial t^*} + \frac{\partial \rho^* u^*}{\partial x^*} = 0, \quad (1)$$

**TABLE I.** Summary of the four dissipation factors in this study and previous studies.<sup>13,18</sup>

	Viscosity of the bubbly liquid	Viscosity at the bubble–liquid interface	Liquid compressibility	Thermal conduction at the bubble–liquid interface
Prosperetti <sup>13</sup>	Not considered	Considered	Not considered	Considered
Kanagawa <i>et al.</i> <sup>18</sup>	Not considered	Considered	Considered	Not considered
This study	Considered	Considered	Considered	Considered

$$\frac{\partial \rho^* u^*}{\partial t^*} + \frac{\partial \rho^* u^{*2}}{\partial x^*} + \frac{\partial p_L^*}{\partial x^*} - \frac{4}{3} \mu^* \frac{\partial^2 u^*}{\partial x^{*2}} = 0, \quad (2)$$

where  $t^*$  is the time,  $x^*$  is the space coordinate,  $\rho^*$  is the density,  $u^*$  is the fluid velocity,  $p^*$  is the pressure, and  $\mu^*$  is the viscosity; the subscript L denotes the liquid phase and  $*$  denotes a dimensional variable. Note that the pressure of the bubbly liquid is equivalent to the averaged pressure of the liquid.<sup>18</sup> Note that (1) and (2) are the volume averaged equations and require the following condition:<sup>2,41,42</sup>

$$R_0^* \ll N_0^{*-1/3} \ll L^*, \quad (3)$$

where  $R_0^*$  is the initial bubble radius,  $N_0^*$  is the initial number density of the bubbles, and  $L^*$  is the typical wavelength.

The bubbly liquid is assumed to be a Newtonian fluid, and the bulk viscosity is ignored based on the Stokes assumption.<sup>43</sup> As proposed in some works,<sup>44,45</sup> the viscosity of the bubbly liquid,  $\mu^*$ , is expressed as follows:

$$\mu^* = (1 + \alpha_0) \mu_L^*, \quad (4)$$

where  $\alpha_0$  is the initial void fraction. Here,  $\mu^*$  is higher than  $\mu_L^*$  because the mechanical work acting on the water is reduced and the velocity of the flow field is reduced due to the containing bubbles.<sup>46</sup> Note that (4) is applicable when  $\alpha_0 < 0.05$ .<sup>47</sup> The volume averaged density of the bubbly liquid,  $\rho^*$ , is defined as

$$\rho^* = (1 - \alpha) \rho_L^*, \quad (5)$$

where  $\alpha$  is the void fraction, and the density of the gas is neglected. The void fraction  $\alpha$  is associated with the number density of the bubbles,  $N^*$ , through the following equation:

$$\alpha = \frac{4}{3} \pi R^{*3} N^*, \quad (6)$$

$$\frac{\partial N^*}{\partial t^*} + \frac{\partial N^* u^*}{\partial x^*} = 0, \quad (7)$$

where  $R^*$  is a representative bubble radius. Equation (6) defines the void fraction,  $\alpha$ , and (7) represents the conservation of the number density of the bubbles,  $N^*$ .

Substituting (6) and (16) below into (7), and (5) into (1) and (2) gives

$$\frac{\partial}{\partial t^*} (\alpha \rho_G^*) + \frac{\partial}{\partial x^*} (\alpha \rho_G^* u^*) = 0, \quad (8)$$

$$\frac{\partial}{\partial t^*} [(1 - \alpha) \rho_L^*] + \frac{\partial}{\partial x^*} [(1 - \alpha) \rho_L^* u^*] = 0, \quad (9)$$

$$\begin{aligned} \frac{\partial}{\partial t^*} [(1 - \alpha) \rho_L^* u^*] + \frac{\partial}{\partial x^*} [(1 - \alpha) \rho_L^* u^{*2}] \\ + \frac{\partial p_L^*}{\partial x^*} - \frac{4}{3} \mu^* \frac{\partial^2 u^*}{\partial x^{*2}} = 0, \end{aligned} \quad (10)$$

where the subscript G denotes the gas phase.

To examine the thermal effect inside the bubble, we use the following relationship at the bubble–liquid interface, proposed by Prosperetti:<sup>13</sup>

$$\frac{Dp_G^*}{Dt^*} = \frac{3}{R^*} \left[ (\kappa - 1) \lambda_G^* \frac{\partial T_G^*}{\partial r^*} \Big|_{r^*=R^*} - \kappa p_G^* \frac{DR^*}{Dt^*} \right], \quad (11)$$

where  $T_G^*$  is the gas temperature,  $\lambda_G^*$  is the thermal conductivity of the gas inside the bubble and  $\kappa$  is the ratio of specific heats. Note that  $R^*$  is not  $R^*(t^*)$ , but  $R^*(t^*, x^*)$ ; the bubble radius is regarded as a field variable defined in all  $t^*$  and  $x^*$ .<sup>48</sup> Note that  $p_G^*$ ,  $T_G^*$ , and  $R^*$  do not depend only on the time  $t^*$  but also on the space  $x^*$ , e.g.,  $p_G^*(t, x)$ . We regard the temperature-gradient  $\partial T_G^* / \partial r^*|_{r^*=R^*}$  as field variables. Further, (11) was recently extended to describe a nonuniform temperature distribution inside the bubble by Zhou & Prosperetti.<sup>49</sup>

The Keller equation for spherical oscillations of a bubble in a compressible liquid is given as follows:<sup>50</sup>

$$\begin{aligned} \left( 1 - \frac{1}{c_{L0}^*} \frac{DR^*}{Dt^*} \right) R^* \frac{D^2 R^*}{Dt^{*2}} + \frac{3}{2} \left( 1 - \frac{1}{3c_{L0}^*} \frac{DR^*}{Dt^*} \right) \left( \frac{DR^*}{Dt^*} \right)^2 \\ = \left( 1 + \frac{1}{c_{L0}^*} \frac{DR^*}{Dt^*} \right) \frac{P^*}{\rho_{L0}^*} + \frac{R^*}{\rho_{L0}^* c_{L0}^*} \frac{D}{Dt^*} (p_L^* + P^*), \end{aligned} \quad (12)$$

where  $P^*$  is the liquid pressure averaged on the bubble–liquid interface,  $c_{L0}^*$  is the sound speed in the initial unperturbed pure water, the subscript 0 denotes the initial unperturbed state, and the material differential operator,  $D/Dt^*$  stands for the following differential operator:

$$\frac{D}{Dt^*} = \frac{\partial}{\partial t^*} + u^* \frac{\partial}{\partial x^*}. \quad (13)$$

To close the set represented in (8)–(12), we introduce the following equations:

(i) Tait's equation of state for liquid,

$$p_L^* = p_{L0}^* + \frac{\rho_{L0}^* c_{L0}^{*2}}{n} \left[ \left( \frac{\rho_L^*}{\rho_{L0}^*} \right)^n - 1 \right]. \quad (14)$$

(ii) Equation of state for ideal gas,

$$\frac{p_G^*}{\rho_{G0}^*} = \frac{\rho_G^*}{\rho_{G0}^*} \frac{T_G^*}{T_0^*}. \quad (15)$$

(iii) Conservation equation of mass inside the bubble,

$$\frac{\rho_G^*}{\rho_{G0}^*} = \left( \frac{R_0^*}{R^*} \right)^3. \quad (16)$$

(iv) Balance of normal stresses across the bubble–liquid interface,

$$p_G^* - (p_L^* + P^*) = \frac{2\sigma^*}{R^*} + \frac{4\mu_L^*}{R^*} \frac{DR^*}{Dt^*}, \quad (17)$$

where  $\sigma^*$  is the surface tension.

## C. Temperature-gradient model

In this study, we not only incorporate the thermal conductivity at the bubble–liquid interface by introducing (11) but also examine the effect of the thermal conductivity resulting from the differences among the temperature-gradient models  $\partial T_G^* / \partial r^*|_{r^*=R^*}$  in the first term on the right-hand side of (11). We use the following four models:<sup>51–54</sup>

(i) Shimada *et al.* (SMK) model,<sup>51</sup>

$$\left. \frac{\partial T_G^*}{\partial r^*} \right|_{r^*=R^*} = \frac{5}{4} \frac{T_0^* - T_G^*}{R^*}. \quad (18)$$

(ii) Lertnuwat *et al.* (LSM) model,<sup>52</sup>

$$\left. \frac{\partial T_G^*}{\partial r^*} \right|_{r^*=R^*} = \frac{T_0^* - T_G^*}{\sqrt{2\pi D^*/\omega_B^*}}. \quad (19)$$

(iii) Preston *et al.* (PCB) model,<sup>53</sup>

$$\left. \frac{\partial T_G^*}{\partial r^*} \right|_{r^*=R^*} = \frac{T_0^* - T_G^*}{|\tilde{L}_p^*|}. \quad (20)$$

(iv) Sugiyama *et al.* (STM) model,<sup>54</sup>

$$\left. \frac{\partial T_G^*}{\partial r^*} \right|_{r^*=R^*} = \frac{\text{Re}(\tilde{L}_p^*)(T_0^* - T_G^*)}{|\tilde{L}_p^*|^2} + \frac{\text{Im}(\tilde{L}_p^*)}{\omega_B^* |\tilde{L}_p^*|^2} \frac{DT_G^*}{Dt^*}, \quad (21)$$

where  $T_0^*$  is the initial temperature,  $D^*$  is the thermal diffusivity of the gas inside the bubble, and Re and Im denote the real and imaginary parts, respectively. Here  $\omega_B^*$  is the natural frequency of a single bubble and is given as follows:<sup>54</sup>

$$\omega_B^* = \sqrt{\frac{3\gamma_e p_{G0}^* - 2\sigma^*/R_0^*}{\rho_{L0}^* R_0^{*2}} - \left( \frac{2\mu_{e0}^*}{\rho_{L0}^* R_0^{*2}} \right)^2}, \quad (22)$$

$$\gamma_e = \text{Re} \left( \frac{\Gamma_N}{3} \right), \quad (23)$$

$$\mu_{e0}^* = \mu_L^* + \text{Im} \left( \frac{p_{G0}^* \Gamma_N}{4\omega_B^*} \right), \quad (24)$$

where  $\gamma_e$  is the effective polytropic exponent; we do not assume explicitly  $\gamma_e$ , except for Sec. IV. Furthermore, we consider  $\mu_{e0}^*$  as the initial effective viscosity. The explicit form of (22) is different from that used in our previous studies.<sup>17,18,21,25–27,31,32,37</sup>

Moreover, the complex number  $\Gamma_N$  is given as<sup>54</sup>

$$\Gamma_N = \frac{3\alpha_N^2 \kappa}{\alpha_N^2 + 3(\kappa - 1)(\alpha_N \coth \alpha_N - 1)}, \quad (25)$$

$$\alpha_N = \sqrt{\frac{\kappa \omega_B^* p_{G0}^* R_0^{*2}}{2(\kappa - 1) T_0^* \lambda_G^*}} (1 + i), \quad (26)$$

where  $\alpha_N$  is also a complex number and  $i$  denotes the imaginary unit. Therefore,  $\tilde{L}_p^*$  in (20) and (21) is the complex number having the dimension of length and is given by

$$\tilde{L}_p^* = \frac{R_0^*(\alpha_N^2 - 3\alpha_N \coth \alpha_N + 3)}{\alpha_N^2(\alpha_N \coth \alpha_N - 1)}. \quad (27)$$

Although the validity of LSM model (19) is confirmed in the range  $R_0^* = O(10^{-5} \text{ m})$ , we use the LSM model (19) in the range  $10^{-5} \text{ m} \leq R_0^* \leq 10^{-3} \text{ m}$ . Let us summarize the main features of (18)–(21) in Table II.

## D. Multiple scale analysis

The time  $t^*$ , and space coordinate  $x^*$  are nondimensionalized using  $t = \omega^* t^*$  and  $x = x^*/L^*$ , respectively, where  $\omega^*$  is the typical angular frequency of a wave and  $L^*$  is the typical wavelength.

Next, we introduce new independent variables based on the typical dimensionless amplitude of a wave  $\varepsilon$  ( $\ll 1$ ) for the near field [i.e., the temporal and spatial scales of  $O(1)$ ] and far field [i.e., the temporal and spatial scales of  $O(1/\varepsilon)$ ],<sup>10</sup>

$$\begin{cases} t_0 = t, & x_0 = x, \\ t_1 = \varepsilon t, & x_1 = \varepsilon x. \end{cases} \quad (28)$$

The dependent variables are nondimensionalized and expanded in powers of  $\varepsilon$ ,

$$\frac{R^*}{R_0^*} - 1 = \varepsilon R_1 + \varepsilon^2 R_2 + O(\varepsilon^3), \quad (29)$$

$$\frac{\alpha}{\alpha_0} - 1 = \varepsilon \alpha_1 + \varepsilon^2 \alpha_2 + O(\varepsilon^3), \quad (30)$$

$$\frac{T_G^*}{T_0^*} - 1 = \varepsilon T_{G1} + \varepsilon^2 T_{G2} + O(\varepsilon^3), \quad (31)$$

$$\frac{u^*}{U^*} = \varepsilon u_1 + \varepsilon^2 u_2 + O(\varepsilon^3), \quad (32)$$

where  $U^*$  is the typical propagation speed of a wave. In the following, nondimensional expressions  $T = T_G^*/T_0^*$  and  $R = R^*/R_0^*$  are also used. The expansion of the liquid density in  $\varepsilon$  is given as follows:<sup>18</sup>

TABLE II. Summary of the main features of temperature-gradient models.

	Main features
Shimada <i>et al.</i> <sup>51</sup>	Estimated a steady-state solution of the temperature-gradient at the bubble–liquid interface when there is a uniform heat source inside the bubble.
Lertnuwat <i>et al.</i> <sup>52</sup>	Estimated the thermal penetration length inside the bubble.
Preston <i>et al.</i> <sup>53</sup>	Modeled strictly based on linear theory.
Sugiyama <i>et al.</i> <sup>54</sup>	Modeled based on the PCB model (20) and incorporated the nonlinearity of bubble oscillation and a phase difference between the average temperature inside the bubble and the temperature-gradient at the bubble–liquid interface.

$$\frac{\rho_L^*}{\rho_{L0}^*} = 1 + \varepsilon^2 \rho_{L1} + \varepsilon^3 \rho_{L2} + O(\varepsilon^4), \quad (33)$$

which is determined from (14) and (38). Furthermore, the pressures are nondimensionalized as

$$p_L = \frac{p_L^*}{\rho_{L0}^* U^{*2}}, \quad p_{L0} = \frac{p_{L0}^*}{\rho_{L0}^* U^{*2}}, \quad p_{G0} = \frac{p_{G0}^*}{\rho_{L0}^* U^{*2}}, \quad (34)$$

where  $p_L$ ,  $p_{L0}$ , and  $p_{G0}$  are  $O(1)$ ;  $p_L$  is expanded as

$$p_L = p_{L0} + \varepsilon p_{L1} + \varepsilon^2 p_{L2} + O(\varepsilon^3). \quad (35)$$

Furthermore, the nondimensional liquid viscosity and initial effective viscosity are defined using  $\varepsilon$ ,

$$\frac{\mu_L^*}{\rho_{L0}^* U^* L^*} = \mu_L \varepsilon, \quad (36)$$

$$\frac{\mu_{e0}^*}{\rho_{L0}^* U^* L^*} = \mu_{e0} \varepsilon, \quad (37)$$

where  $\mu_L$  and  $\mu_{e0}$  are constants of  $O(1)$ . In addition, there exists a relationship  $U^* = L^* \omega^*$  among  $U^*$ ,  $L^*$ , and  $\omega^*$ , and we determine the values of the three nondimensionalized ratios as follows.<sup>17,18,42</sup>

$$\left( \frac{U^*}{c_{L0}^*}, \frac{R_0^*}{L^*}, \frac{\omega^*}{\omega_B^*} \right) = (V\sqrt{\varepsilon}, \Delta\sqrt{\varepsilon}, \Omega\sqrt{\varepsilon}), \quad (38)$$

where  $V$ ,  $\Delta$ , and  $\Omega$  are constants of  $O(1)$ .

### E. Nondimensionalization of energy equation (11)

Equation (11) is nondimensionalized as

$$\frac{D}{Dt} [T_G R^{3(\kappa-1)}] = R^{3\kappa-1} \frac{3(\kappa-1)\lambda_G^*}{p_{G0}^* \omega_B^* R_0^*} \frac{\partial T^*}{\partial r^*} \bigg|_{r=R^*}. \quad (39)$$

The nondimensionalized expression on the right-hand side of (39) depends on which temperature-gradient models we choose. First, in the case of (18),

$$(\text{RHS}) = \frac{3(\kappa-1)\lambda_G^*}{p_{G0}^* \omega_B^* R_0^*} \frac{5}{4} \frac{T_0^*}{R_0^*} R^{3\kappa-2} (1 - T_G), \quad (40)$$

and then, we determine the sizes of the nondimensional ratio in (40) using  $\varepsilon$  as follows:

$$\frac{3(\kappa-1)\lambda_G^*}{p_{G0}^* \omega_B^* R_0^*} \frac{5}{4} \frac{T_0^*}{R_0^*} \equiv \zeta_{\text{SMK}} \varepsilon. \quad (41)$$

In the same manner, we also determine the sizes of the nondimensional ratios in the other cases: In (19),

$$(\text{RHS}) = \frac{3(\kappa-1)\lambda_G^*}{p_{G0}^* \omega_B^* R_0^*} \frac{T_0^*}{\sqrt{2\pi D^* / \omega_B^*}} R^{3\kappa-1} (1 - T_G), \quad (42)$$

$$\frac{3(\kappa-1)\lambda_G^*}{p_{G0}^* \omega_B^* R_0^*} \frac{T_0^*}{\sqrt{2\pi D^* / \omega_B^*}} \equiv \zeta_{\text{LSM}} \varepsilon. \quad (43)$$

In (20),

$$(\text{RHS}) = \frac{3(\kappa-1)\lambda_G^*}{p_{G0}^* \omega_B^* R_0^*} \frac{T_0^*}{|\tilde{L}_P^*|} R^{3\kappa-1} (1 - T_G), \quad (44)$$

$$\frac{3(\kappa-1)\lambda_G^*}{p_{G0}^* \omega_B^* R_0^*} \frac{T_0^*}{|\tilde{L}_P^*|} \equiv \zeta_{\text{PCB}} \varepsilon. \quad (45)$$

In (21),

$$(\text{RHS}) = \frac{3(\kappa-1)\lambda_G^*}{p_{G0}^* \omega_B^* R_0^*} R^{3\kappa-1} \left[ \frac{\text{Re}(\tilde{L}_P^*) T_0^*}{|\tilde{L}_P^*|^2} (1 - T_G) + \frac{\omega^* \text{Im}(\tilde{L}_P^*) T_0^*}{\omega_B^* |\tilde{L}_P^*|^2} \frac{DT_G}{Dt} \right], \quad (46)$$

$$\frac{3(\kappa-1)\lambda_G^*}{p_{G0}^* \omega_B^* R_0^*} \frac{\text{Re}(\tilde{L}_P^*) T_0^*}{|\tilde{L}_P^*|^2} \equiv \zeta_{\text{STM1}} \varepsilon, \quad (47)$$

$$\frac{3(\kappa-1)\lambda_G^*}{p_{G0}^* \omega_B^* R_0^*} \frac{\omega^* \text{Im}(\tilde{L}_P^*) T_0^*}{\omega_B^* |\tilde{L}_P^*|^2} \equiv \zeta_{\text{STM2}} \varepsilon, \quad (48)$$

where  $\zeta_{\text{SMK}}$ ,  $\zeta_{\text{LSM}}$ ,  $\zeta_{\text{PCB}}$ ,  $\zeta_{\text{STM1}}$ , and  $\zeta_{\text{STM2}}$  are constants of  $O(1)$ . Note that (43), (45), (47), and (48) determine the sizes of nondimensional ratios.

## III. DERIVATION OF KdVB EQUATION

This section focuses on the derivation of the KdVB equation, and the discussions will be presented in Sec. IV.

### A. Leading order of approximation

Equating the coefficients of the like powers of  $\varepsilon$  in the governing equations (8)–(12), a set of linearized first-order equations is derived,

$$\frac{\partial \alpha_1}{\partial t_0} - 3 \frac{\partial R_1}{\partial t_0} + \frac{\partial u_1}{\partial x_0} = 0, \quad (49)$$

$$\alpha_0 \frac{\partial \alpha_1}{\partial t_0} - (1 - \alpha_0) \frac{\partial u_1}{\partial x_0} = 0, \quad (50)$$

$$(1 - \alpha_0) \frac{\partial u_1}{\partial t_0} + \frac{\partial p_{L1}}{\partial x_0} = 0, \quad (51)$$

$$\frac{\partial T_{G1}}{\partial t_0} + 3(\kappa - 1) \frac{\partial R_1}{\partial t_0} = 0, \quad (52)$$

$$-\frac{\Delta^2}{\Omega^2} R_1 - p_{L1} + p_{G0} T_1 + 3(\gamma_e - 1) p_{G0} R_1 + \frac{4\mu_{e0}^2}{\Delta^2} = 0. \quad (53)$$

The differences between our previous and present studies are the appearances of the energy equation (52) and the third, fourth, and fifth terms in (53).

We summarize (49)–(53) into the following single partial differential equation for the first-order perturbation of the bubble radius,  $R_1$ ,

$$\frac{\partial^2 R_1}{\partial t_0^2} - v_p^2 \frac{\partial^2 R_1}{\partial x_0^2} = 0, \quad (54)$$

where the phase velocity  $v_p$  is given by

$$v_p = \sqrt{\frac{\Delta^2 + 3(\kappa - \gamma_e)p_{G0}}{3\alpha_0(1 - \alpha_0)}}. \quad (55)$$

Next, setting  $v_p \equiv 1$ , for simplicity, yields

$$U^* = \sqrt{\frac{R_0^{*2}\omega_B^{*2} + 3(\kappa - \gamma_e)p_{G0}^*/\rho_{L0}^*}{3\alpha_0(1 - \alpha_0)}}. \quad (56)$$

We emphasize that the phase velocity  $U^*$  is affected by the effective polytropic exponent  $\gamma_e$  describing thermodynamics inside the bubble, although the phase velocity did not contain  $\gamma_e$  in our previous study [see Eq. (24) in Ref. 18].

In the following, we describe the right-running wave in the leading order of approximation, and a phase function  $\varphi_0$  is introduced as follows:

$$\varphi_0 = x_0 - t_0. \quad (57)$$

With  $R_1 \equiv f(\varphi_0; t_1, x_1)$ , (54) reduces to

$$\frac{\partial f}{\partial t_0} + \frac{\partial f}{\partial x_0} = 0. \quad (58)$$

In the near field, all the first-order perturbations  $\alpha_1$ ,  $u_1$ ,  $T_{G1}$ ,  $p_{L1}$ , and  $R_1$  are governed by (58). Rewriting (49)–(53) using  $\varphi_0$  and integrating them with respect to  $\varphi_0$ , we obtain the following relationships:

$$\alpha_1 = s_1 f, \quad u_1 = s_2 f, \quad T_{G1} = s_3 f, \quad p_{L1} = s_4 f, \quad (59)$$

$$s_1 = 3(1 - \alpha_0), \quad s_2 = -3\alpha_0, \quad s_3 = -3(\kappa - 1), \quad s_4 = -3\alpha_0(1 - \alpha_0). \quad (60)$$

Here, the constants of integration are dropped because of boundary conditions at  $x_0 \rightarrow \infty$ , where the bubbly liquid is uniform and at rest.

## B. Second order of approximation and resultant KdVB equation

The set of second-order equations is expressed as

$$\frac{\partial \alpha_2}{\partial t_0} - 3 \frac{\partial R_2}{\partial t_0} + \frac{\partial u_2}{\partial x_0} = K_1, \quad (61)$$

$$\alpha_0 \frac{\partial \alpha_2}{\partial t_0} - (1 - \alpha_0) \frac{\partial u_2}{\partial x_0} = K_2, \quad (62)$$

$$(1 - \alpha_0) \frac{\partial u_2}{\partial t_0} + \frac{\partial p_{L2}}{\partial x_0} = K_3, \quad (63)$$

$$\frac{\partial T_{G2}}{\partial t_0} + 3(\kappa - 1) \frac{\partial R_2}{\partial t_0} = K_4, \quad (64)$$

$$-\frac{\Delta^2}{\Omega^2} R_2 - p_{L2} + p_{G0} T_2 + 3(\gamma_e - 1) p_{G0} R_2 = K_5, \quad (65)$$

where the inhomogeneous terms  $K_j$  ( $j = 1, 2, 3, 5$ ) are obtained as

$$K_1 = 3 \frac{\partial}{\partial t_0} (\alpha_1 R_1 - 2R_1^2) + \frac{\partial}{\partial x_0} (3u_1 R_1 - \alpha_1 u_1) - \left( \frac{\partial \alpha_1}{\partial t_1} - 3 \frac{\partial R_1}{\partial t_1} + \frac{\partial u_1}{\partial x_1} \right), \quad (66)$$

$$K_2 = (1 - \alpha_0) \frac{\partial p_{L1}}{\partial t_0} - \alpha_0 \frac{\partial \alpha_1 u_1}{\partial x_0} - \left[ \alpha_0 \frac{\partial \alpha_1}{\partial t_1} - (1 - \alpha_0) \frac{\partial u_1}{\partial x_1} \right], \quad (67)$$

$$K_3 = \alpha_0 \frac{\partial \alpha_1 u_1}{\partial t_0} - (1 - \alpha_0) \frac{\partial u_1^2}{\partial x_0} - \left[ (1 - \alpha_0) \frac{\partial u_1}{\partial t_1} + \frac{\partial p_{L1}}{\partial x_1} \right] + \frac{4}{3} (1 + \alpha_0) \mu \frac{\partial^2 u_1}{\partial x_0^2}, \quad (68)$$

$$K_5 = \Delta^2 \frac{\partial^2 R_1}{\partial t_0^2} + 3p_{G0} R_1 T_1 + \frac{4\mu_{e0}^2}{\Delta^2} R_1 - V \Delta \left\{ \left[ 3(\gamma_e - 1) p_{G0} - \frac{\Delta^2}{\Omega^2} \right] \frac{\partial R_1}{\partial t_0} + p_{G0} \frac{\partial T_1}{\partial t_0} \right\} - R_1^2 \left[ 3(2 - \gamma_e) p_{G0} + \frac{\Delta^2}{\Omega^2} \right] + 4\mu \frac{\partial R_1}{\partial t_0}. \quad (69)$$

Here, the explicit form of  $K_4$  depends on which the temperature-gradient models, i.e., (18)–(21), are used:

(i) For the cases of (18)–(20),

$$K_4 = - \left[ \frac{\partial T_{G1}}{\partial t_1} + 3(\kappa - 1) \frac{\partial R_1}{\partial t_1} \right] - u_1 \frac{\partial T_{G1}}{\partial x_0} - 3(\kappa - 1) u_1 \frac{\partial R_1}{\partial x_0} - \frac{3(\kappa - 1)[3(\kappa - 1) - 1]}{2!} \frac{\partial R_1^2}{\partial t_0} - 3(\kappa - 1) \frac{\partial T_{G1} R_1}{\partial t_0} + \zeta T_{G1}. \quad (70)$$

(ii) For the case of (21),

$$K_4 = - \left[ \frac{\partial T_{G1}}{\partial t_1} + 3(\kappa - 1) \frac{\partial R_1}{\partial t_1} \right] - u_1 \frac{\partial T_{G1}}{\partial x_0} - 3(\kappa - 1) u_1 \frac{\partial R_1}{\partial x_0} - \frac{3(\kappa - 1)[3(\kappa - 1) - 1]}{2!} \frac{\partial R_1^2}{\partial t_0} - 3(\kappa - 1) \frac{\partial T_{G1} R_1}{\partial t_0} + \zeta_{STM1} T_{G1} + \zeta_{STM2} \frac{\partial T_{G1}}{\partial t_0}, \quad (71)$$

where  $\zeta$  in (70) represents  $\zeta_{SKM}$ ,  $\zeta_{LSM}$ , and  $\zeta_{PCB}$ . Then, we obtain the inhomogeneous wave equation from the approximation of  $O(\varepsilon^2)$ ,

$$\frac{\partial^2 R_2}{\partial t_0^2} - \frac{\partial^2 R_2}{\partial x_0^2} = K(f; \varphi_0, t_1, x_1) = \frac{\partial}{\partial \varphi_0} \left[ \frac{1}{3} K_1 - \frac{1}{3\alpha_0} K_2 + \frac{1}{3\alpha_0(1 - \alpha_0)} K_3 + \frac{p_{G0}}{3\alpha_0(1 - \alpha_0)} K_4 + \frac{1}{3\alpha_0(1 - \alpha_0)} K_5 \right]. \quad (72)$$

Using the solvability condition<sup>10,17,18</sup> to (72), we finally derive

$$\frac{\partial f}{\partial \tau} + \Pi_1 f \frac{\partial f}{\partial \xi} + \Pi_{21} \frac{\partial^2 f}{\partial \xi^2} + \Pi_{22} f + \Pi_3 \frac{\partial^3 f}{\partial \xi^3} = 0, \quad (73)$$

$$\tau = \varepsilon t, \quad \xi = x - (1 + \varepsilon \Pi_0) t, \quad (74)$$

where  $\tau$  and  $\xi$  are the transformed time and space coordinate, respectively,  $\Pi_0$  is the advection coefficient,  $\Pi_1$  is the nonlinear coefficient,  $\Pi_{21}$  is the dissipation coefficient due to viscosity and acoustic radiation,  $\Pi_{22}$  is the newly obtained dissipation coefficient due to thermal conductivity, and  $\Pi_3$  is the dispersion coefficient.

Moreover, the explicit forms of the coefficients in (73), i.e.,  $\Pi_1$ ,  $\Pi_{21}$ ,  $\Pi_{22}$ , and  $\Pi_3$ , are given as follows:

$$\Pi_1 = \frac{1}{6} \left[ k_1 - \frac{k_2}{\alpha_0} + \frac{k_3}{\alpha_0(1-\alpha_0)} + \frac{p_{G0}k_4}{\alpha_0(1-\alpha_0)} + \frac{k_5}{\alpha_0(1-\alpha_0)} \right] < 0, \quad (75)$$

$$k_1 = 6(2-s_1) + 2s_2(3-s_1), \quad k_2 = -2\alpha_0 s_1 s_2, \quad k_3 = 0, \quad (76)$$

$$k_4 = 6 \left[ 3(\kappa-1)s_3 - \frac{(3\kappa-3)(3\kappa-4)}{2!} \right],$$

$$k_5 = -6 \left[ \frac{\Delta^2}{\Omega^2} + 3(2-\gamma_e-s_3)p_{G0} \right],$$

$$\Pi_{21} = -\frac{1}{6\alpha_0(1-\alpha_0)} \left( -\frac{4}{3}s_2(1+\alpha_0)\mu_L + 4\mu_L + V\Delta \left\{ \frac{\Delta^2}{\Omega^2} - [3(\gamma_e-1)+s_3]p_{G0} \right\} \right) < 0, \quad (77)$$

$$\Pi_{22} = -\frac{p_{G0}}{6\alpha_0(1-\alpha_0)} \zeta s_3 > 0, \quad (78)$$

$$\Pi_3 = \frac{\Delta^2}{6\alpha_0(1-\alpha_0)} > 0, \quad (79)$$

where  $\zeta$  represents  $\zeta_{SKM}$ ,  $\zeta_{LSM}$ ,  $\zeta_{PCB}$ , and  $\zeta_{STM1}$ . Remarking that  $\Pi_1$ ,  $\Pi_{22}$ , and  $\Pi_3$  do not depend on  $\alpha_0$  but depend on  $R_0^*$ . The explicit form of the advection coefficient,  $\Pi_0$ , depends on the temperature-gradient models:

(i) For the cases of (18)–(20),

$$\Pi_0 = \frac{2\mu_{e0}^2}{3\alpha_0(1-\alpha_0)\Delta^2} - \frac{(1-\alpha_0)^2 V^2}{2}. \quad (80)$$

(ii) For the case of (21),

$$\Pi_0 = \frac{2\mu_{e0}^2}{3\alpha_0(1-\alpha_0)\Delta^2} - \frac{p_{G0}}{6\alpha_0(1-\alpha_0)} \zeta_{STM2} s_3 - \frac{(1-\alpha_0)^2 V^2}{2}. \quad (81)$$

As shown in (80) and (81), the initial effective viscosity is included in the natural frequency (22), newly introduced in this study. Furthermore, when we use model (21), the coefficient  $\Pi_0$  included the phase difference between the temperature gradient,  $\partial T_G^*/\partial r^*|_{r=R^*}$ , and the average temperature inside the bubble,  $T_G^*$ .<sup>54</sup>

#### IV. DISCUSSION

In this section, we discuss the differences among the present study and two previous studies (i.e., Refs. 13 and 18). Before the discussion, we introduce the KdVB equations derived in the previous studies.<sup>13,18</sup>

The one derived in our previous study<sup>18</sup> is given by

$$\frac{\partial f}{\partial \tau} + \widetilde{\Pi}_1 f \frac{\partial f}{\partial \xi} + \widetilde{\Pi}_2 \frac{\partial^2 f}{\partial \xi^2} + \widetilde{\Pi}_3 \frac{\partial^3 f}{\partial \xi^3} = 0, \quad (82)$$

$$\tau = \varepsilon t, \quad \xi = x - (1 + \varepsilon \widetilde{\Pi}_0) t, \quad (83)$$

with

$$\widetilde{\Pi}_0 = -\frac{(1-\alpha_0)^2 V^2}{2}, \quad (84)$$

$$\widetilde{\Pi}_1 = \frac{1}{6} \left[ \widetilde{k}_1 - \frac{\widetilde{k}_2}{\alpha_0} + \frac{\widetilde{k}_3}{\alpha_0(1-\alpha_0)} + \widetilde{k}_4 + 6\widetilde{k}_5 \right] < 0, \quad (85)$$

$$\widetilde{\Pi}_2 = -\frac{1}{6\alpha_0(1-\alpha_0)} \left( 4\mu_L + \frac{V\Delta^3}{\Omega^2} \right) < 0, \quad (86)$$

$$\widetilde{\Pi}_3 = \frac{\Delta^2}{6\alpha_0(1-\alpha_0)} > 0, \quad (87)$$

where  $\widetilde{k}_j$  ( $j = 1, 2, \dots, 5$ ) are given by

$$\begin{aligned} \widetilde{k}_1 &= k_1, & \widetilde{k}_2 &= k_2, & \widetilde{k}_3 &= k_3 = 0, & \widetilde{k}_4 &= 0, \\ \widetilde{k}_5 &= 1 + \frac{\gamma(3\gamma-1)p_{G0}}{2\alpha_0(1-\alpha_0)}. \end{aligned} \quad (88)$$

In our previous study,<sup>18</sup> we did not use  $\gamma_e$  but used  $\gamma$  and did not consider thermal conductivity. In the following, we express the quantity obtained in our previous study<sup>18</sup> using the symbol  $\sim$ .

Furthermore, we use Prosperetti's equation<sup>13</sup> as the other KdVB equation,

$$\frac{\partial f}{\partial \tau} + \widehat{\Pi}_1 f \frac{\partial f}{\partial \xi} + \widehat{\Pi}_2 \frac{\partial^2 f}{\partial \xi^2} + \widehat{\Pi}_3 \frac{\partial^3 f}{\partial \xi^3} = 0, \quad (89)$$

$$\tau = \varepsilon t, \quad \xi = x - t, \quad (90)$$

with

$$\widehat{\Pi}_1 = -\left( 1 + \frac{6-w}{2\psi^2} \right) < 0, \quad (91)$$

$$\widehat{\Pi}_2 = -\frac{1}{\varepsilon\psi^2} \left( M + \frac{1}{2} \frac{\kappa-1}{5\kappa\delta} \right) < 0, \quad (92)$$

$$\widehat{\Pi}_3 = \frac{Y^2}{2\varepsilon\psi^2} > 0, \quad (93)$$

where  $w$ ,  $\psi^2$ ,  $M$ ,  $\delta$ , and  $Y^2$  are the nondimensional numbers defined in Eqs. (2.20), (7.8), (2.22), (2.14), and (7.21) of Prosperetti's paper,<sup>13</sup> respectively (see the detailed definitions and explanations in Ref. 13); the other symbols (i.e.,  $f$ ,  $\tau$ ,  $\xi$ ,  $x$ ,  $t$ ,  $\varepsilon$ , and  $\kappa$ ) are the same as those in the present study. In the following, we express the original coefficients obtained in Prosperetti's study<sup>13</sup> as the symbol  $\widehat{\cdot}$ . Note that coefficients (90) and (91) assuming an isothermal case are used because the analytically explicit expression of coefficients is impossible for an adiabatic case (see the detailed explanation in Ref. 13).

#### A. Effective polytropic exponent

In this study, Fig. 1 shows the dependence of the effective polytropic exponent,  $\gamma_e$ , on the initial bubble radius,  $R_0^*$ . For small  $R_0^*$ , the thermodynamic processes occurring inside the bubble become isothermal (i.e.,  $\gamma_e \rightarrow 1$ ), and for large  $R_0^*$ , the processes become adiabatic (i.e.,  $\gamma_e \rightarrow \kappa$ ).

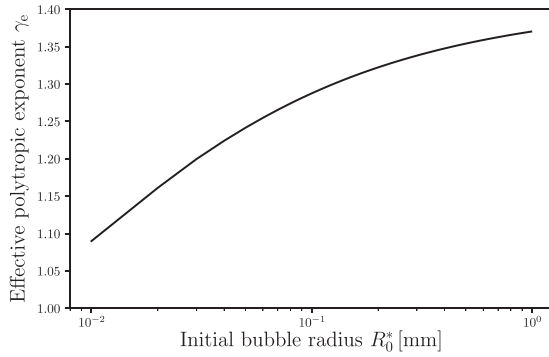


**FIG. 1.** Dependence of the effective polytropic exponent  $\gamma_e$  on the initial bubble radius  $R_0^*$  for  $\Omega = 1$ ,  $\sqrt{\varepsilon} = 0.15$ ,  $\alpha_0 = 0.05$ ,  $\rho_{L0}^* = 101325$  Pa,  $\rho_{L0}^* = 1000$  kg/m<sup>3</sup>,  $\sigma^* = 0.0728$  N/m,  $c_{L0}^* = 1500$  m/s,  $\mu_L^* = 1 \times 10^{-3}$  Pa · s, and  $\lambda_G^* = 0.0241$  W/(m · K). The same condition is used in Figs. 2–10.

## B. Dispersion coefficient

Figure 2 shows the dependence of the dispersion coefficients, namely, the present coefficient  $\Pi_3$  and our previous coefficient<sup>18</sup>  $\tilde{\Pi}_3$  on  $R_0^*$ . As  $\tilde{\Pi}_3 = \Pi_3$ , Prosperetti's coefficient<sup>13</sup>  $\hat{\Pi}_3$  is omitted in Fig. 2. While  $\tilde{\Pi}_3$  is constant,  $\Pi_3$  depends on  $R_0^*$ .

## C. Nonlinear coefficient

First, we compare our present coefficient  $\Pi_1$  with our previous coefficient<sup>18</sup>  $\tilde{\Pi}_1$ . Figure 3 shows the dependence of the nonlinear coefficients,  $\Pi_1$  and  $\tilde{\Pi}_1$  on  $R_0^*$ ,  $|\Pi_1|$  is larger than  $|\tilde{\Pi}_1|$ . We decompose  $\Pi_1$  and  $\tilde{\Pi}_1$  into

$$\Pi_1 = \pi_1 + \pi_2 + \pi_3 + \pi_4 + \pi_5, \quad (94)$$

$$\tilde{\Pi}_1 = \tilde{\pi}_1 + \tilde{\pi}_2 + \tilde{\pi}_3 + \tilde{\pi}_4 + \tilde{\pi}_5, \quad (95)$$

with

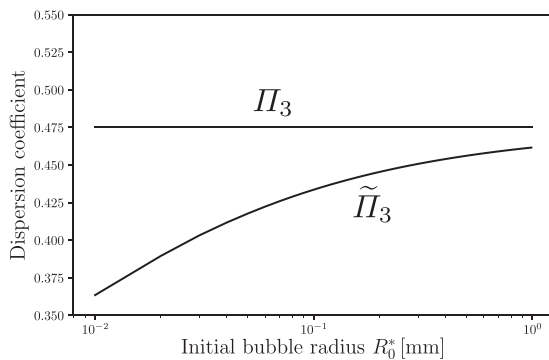


**FIG. 2.** Dependence of the dispersion coefficients  $\Pi_3$  and  $\tilde{\Pi}_3$  on  $R_0^*$ .

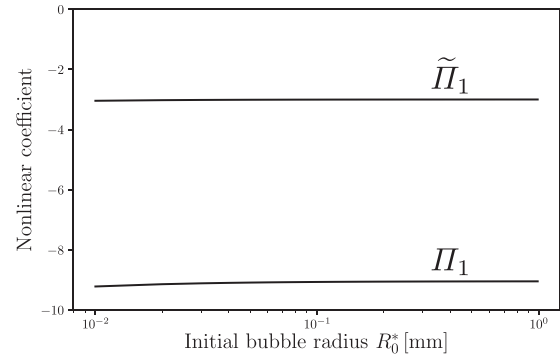


**FIG. 3.** Dependence of nonlinear coefficients  $\Pi_1$  and  $\tilde{\Pi}_1$  on  $R_0^*$ .

$$\pi_1 = \frac{k_1}{6}, \quad \pi_2 = -\frac{k_2}{6\alpha_0}, \quad \pi_3 = \frac{k_3}{6\alpha_0(1-\alpha_0)}, \quad (96)$$

$$\pi_4 = \frac{p_{G0}k_4}{6\alpha_0(1-\alpha_0)}, \quad \pi_5 = \frac{k_5}{6\alpha_0(1-\alpha_0)},$$

$$\tilde{\pi}_1 = \frac{\tilde{k}_1}{6}, \quad \tilde{\pi}_2 = \frac{\tilde{k}_2}{6\alpha_0}, \quad \tilde{\pi}_3 = \frac{\tilde{k}_3}{6\alpha_0(1-\alpha_0)}, \quad (97)$$

$$\tilde{\pi}_4 = \frac{\tilde{k}_4}{6}, \quad \tilde{\pi}_5 = \tilde{k}_5.$$

Here,  $\pi_j$  and  $\tilde{\pi}_j$  ( $j = 1, 2, \dots, 5$ ) represent the nonlinear effect of the basic equations (8)–(12) [i.e., the conservation of number density (8), mass (9), momentum (10), and energy (11), and bubble dynamics (12)] on  $\Pi_1$  and  $\tilde{\Pi}_1$ . Note that (i)  $\pi_j = \tilde{\pi}_j$  ( $j = 1, 2, 3$ ); (ii) the momentum conservation equation does not affect the nonlinearity because  $\pi_3 = \tilde{\pi}_3 = 0$  ( $k_3 = 0$ ); (iii) as thermal conduction was not incorporated in our previous study,<sup>18</sup>  $\tilde{\pi}_4 = 0$ .

Figure 4 shows each contribution of  $\pi_j$  and  $\tilde{\pi}_j$  ( $j = 1, 2, \dots, 5$ ) to the nonlinear coefficients,  $\Pi_1$  and  $\tilde{\Pi}_1$ . The present nonlinearity (i.e., absolute value of nonlinear coefficient) increases owing to the introduction of  $\pi_4$  and the increase in  $\pi_5$ , resulting from the introduction of (11) and the incorporation of the temperature variation inside the bubbles to (15). Second, we compare our present coefficient  $\Pi_1$ , our previous coefficient<sup>18</sup>  $\tilde{\Pi}_1$ , and Prosperetti's coefficient<sup>13</sup>  $\hat{\Pi}_1$ . Figure 5 shows the dependence of the nonlinear coefficients, the present coefficient  $\Pi_1$ , and Prosperetti's coefficient<sup>13</sup>  $\hat{\Pi}_1$  on  $R_0^*$ ,  $|\Pi_1|$  is larger than  $|\hat{\Pi}_1|$ .

## D. Effect of viscosity and compressibility on dissipation coefficient

Here, we present the most important discussion, i.e., dissipation coefficient. As summarized in Table I, dissipation factors considered are the viscosity, liquid compressibility (i.e., acoustic radiation), and thermal conduction. Our present KdVB equation (73) comprises two types of dissipation coefficients: One is the coefficient of the well-known second-order derivative with respect to the space,  $\Pi_{21}$ , which includes the effects of the viscosity of the bubbly liquid, liquid viscosity at the bubble–liquid interface, and liquid compressibility. The other is

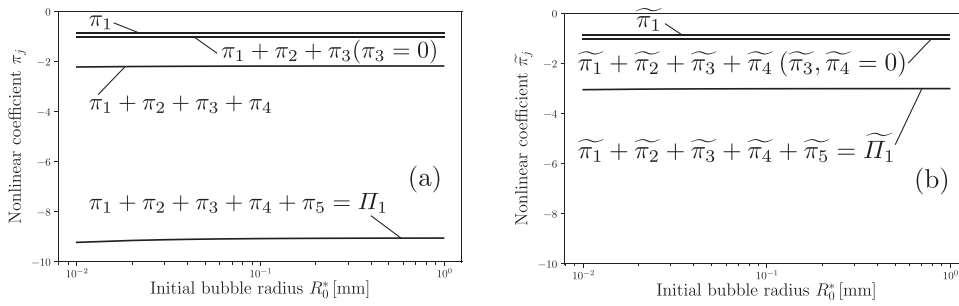


**FIG. 4.** Contribution of each basic equation to nonlinear coefficients (a)  $\Pi_1$  and (b)  $\tilde{\Pi}_1$ ;  $\pi_j$  and  $\tilde{\pi}_j$  ( $j = 1, 2, \dots, 5$ ) correspond to the conservation of number density (8), mass (9), momentum (10), and energy (11), and bubble dynamics (12) in basic equations, respectively.

the newly discovered coefficient of the term without differentiation,  $\Pi_{22}$ , which includes the effect of thermal conduction. Both previous studies (Refs. 13 and 18) derived only the coefficients of the second-order derivatives with respect to the space,  $\tilde{\Pi}_2$  and  $\hat{\Pi}_2$ . Our previous coefficient  $\tilde{\Pi}_2$  included the effects of the liquid viscosity at the bubble-liquid interface and acoustic radiation, whereas Prosperetti's coefficient  $\hat{\Pi}_2$  included the effects of the liquid viscosity at the bubble-liquid interface and thermal conductivity.

Next, we discuss each dissipation factor. The three dissipation coefficients are decomposed into

$$\Pi_{21} = \pi_{\text{vis}} + \pi_{\text{ac}}, \quad (98)$$

$$\pi_{\text{vis}} = -\frac{1}{6\alpha_0(1-\alpha_0)} \left[ -\frac{4}{3}s_2(1+\alpha_0)\mu_L + 4\mu_L \right], \quad (99)$$

$$\pi_{\text{ac}} = -\frac{V\Delta}{6\alpha_0(1-\alpha_0)} \left\{ \frac{\Delta^2}{\Omega^2} - [3(\gamma_e - 1) + s_3]p_{G0} \right\},$$

$$\tilde{\Pi}_2 = \tilde{\pi}_{\text{vis}} + \tilde{\pi}_{\text{ac}}, \quad (100)$$

$$\tilde{\pi}_{\text{vis}} = -\frac{4\mu_L}{6\alpha_0(1-\alpha_0)}, \quad (101)$$

$$\tilde{\pi}_{\text{ac}} = -\frac{1}{6\alpha_0(1-\alpha_0)} \frac{V\Delta^3}{\Omega^2},$$

$$\hat{\Pi}_2 = \hat{\pi}_{\text{vis}} + \hat{\pi}_{\text{th}}, \quad (102)$$

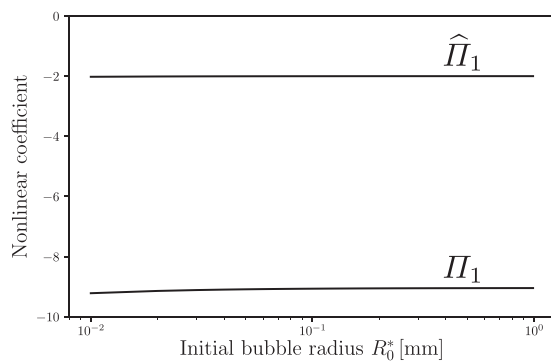


**FIG. 5.** Dependence of nonlinear coefficients  $\Pi_1$  and  $\tilde{\Pi}_1$  on  $R_0^*$ .

$$\hat{\pi}_{\text{vis}} = -\frac{M}{\varepsilon\psi^2}, \quad \hat{\pi}_{\text{th}} = -\frac{1}{2\varepsilon\psi^2} \frac{\kappa - 1}{5\kappa\delta}, \quad (103)$$

where the subscripts “vis,” “ac,” and “th” represent the viscosity, acoustic radiation, and thermal conduction, respectively.

Figure 6 shows the dependence of the dissipation effects due to viscosity, i.e.,  $\pi_{\text{vis}}$ ,  $\tilde{\pi}_{\text{vis}}$ , and  $\hat{\pi}_{\text{vis}}$  on  $R_0^*$ ;  $\pi_{\text{vis}}$ ,  $\tilde{\pi}_{\text{vis}}$ , and  $\hat{\pi}_{\text{vis}}$  decrease as  $R_0^*$  increases. Further,  $|\pi_{\text{vis}}| < |\tilde{\pi}_{\text{vis}}|$  is always satisfied. The effect of viscosity of bubbly liquids is significantly smaller than that of the viscosity at the bubble-liquid interface. Figure 7 shows the dependence of the dissipation effects due to acoustic radiation, i.e.,  $\pi_{\text{ac}}$  and  $\tilde{\pi}_{\text{ac}}$ , on  $R_0^*$ ;  $|\pi_{\text{ac}}| > |\tilde{\pi}_{\text{ac}}|$  is always satisfied. In addition,  $O(\pi_{\text{ac}}) = O(\pi_{\text{vis}})$ .

### E. Effect of thermal conduction on dissipation coefficient: Difference among four temperature-gradient models

We now discuss the newly discovered coefficient  $\Pi_{22}$  in (73) focusing on the differences among the temperature-gradient models [i.e., SMK (18),<sup>51</sup> LSM (19),<sup>52</sup> PCB (20),<sup>53</sup> and STM (21)<sup>54</sup>]. Figure 8 shows the dependence of the dissipation effect due to thermal conduction  $\Pi_{22}$  on  $R_0^*$  considering the four models used;  $\Pi_{22}$  decreases as  $R_0^*$  increases for every model. The difference among the four models is small for the milliscal bubbles. However, for microscale bubbles, the values in the PCB and STM

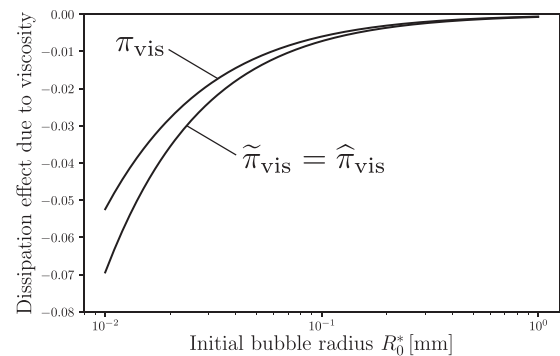


**FIG. 6.** Dependence of dissipation effects due to viscosity  $\pi_{\text{vis}}$ ,  $\tilde{\pi}_{\text{vis}}$ , and  $\hat{\pi}_{\text{vis}}$  on  $R_0^*$ .

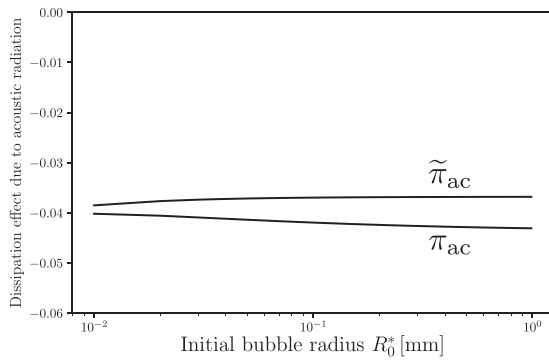


FIG. 7. Dependence of dissipation effects due to acoustic radiation  $\pi_{ac}$  and  $\tilde{\pi}_{ac}$  on  $R_0^*$ .

models are high compared with those in the LSM and SMK models; the PCB model is similar to the STM model, and the LSM model is to the SMK model. The absolute value of  $\Pi_{22}$  is significantly higher than that of  $\Pi_{21}$ .

#### F. Effect of thermal conduction on dissipation coefficient: Comparison of two types of dissipation terms by numerical analysis

Now, we compare the present thermal dissipation coefficient,  $\Pi_{22}$ , with  $\hat{\pi}_{th}$ , the component of thermal dissipation in coefficient,  $\hat{\Pi}_2$  proposed by Prosperetti;<sup>13</sup> our previous study<sup>18</sup> neglected thermal conduction. However, while  $\hat{\Pi}_2$  is the coefficient of the term without differentiation,  $\hat{\pi}_{th}$  is the coefficient of the second-order derivative, as shown in (73) and (89), respectively. Therefore, comparing the difference between coefficients  $\hat{\Pi}_2$  and  $\hat{\pi}_{th}$  is meaningless from the viewpoint of the size of thermal dissipation (not dissipation coefficient). Then, we numerically analyze  $\Pi_{22}p_{L1}$  and  $\hat{\pi}_{th}\partial^2 p_{L1}/\partial \xi^2$  using the spatio-temporal evolution of the unknown

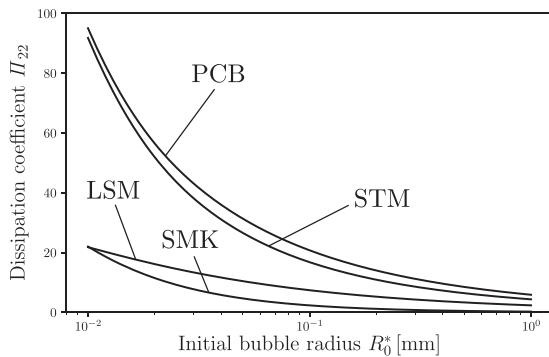


FIG. 8. Dependence of the dissipation coefficient due to thermal conduction  $\Pi_{22}$  on  $R_0^*$ . The four temperature-gradient models, i.e., SMK (18),<sup>51</sup> LSM (19),<sup>52</sup> PCB (20),<sup>53</sup> and STM (21),<sup>54</sup> are used.

variable,  $p_{L1}$ , numerically obtained as the solution of the KdVB equation. The numerical scheme is presented in the Appendix.

Figure 9 shows the result of temporal evolution of the present thermal dissipation  $\Pi_{22}p_{L1}$  and that determined by Prosperetti<sup>13</sup>  $\hat{\pi}_{th}\partial^2 p_{L1}/\partial \xi^2$ . The order of  $\Pi_{22}p_{L1} = O(10^{-1})$  is comparable with that of  $\hat{\pi}_{th}\partial^2 p_{L1}/\partial \xi^2$ , although the mathematical forms of the dissipation terms differ in each study. It is implied that our newly discovered thermal dissipation term, i.e.,  $\Pi_{22}p_{L1}$ , physically agrees with the thermal dissipation term determined by Prosperetti,<sup>13</sup> i.e.,  $\hat{\pi}_{th}\partial^2 p_{L1}/\partial \xi^2$ , from the viewpoint of the order.

Figure 10 also shows the temporal evolution of the present thermal dissipation  $\Pi_{22}p_{L1}$  and the present dissipation by the viscosity and acoustic radiation  $\Pi_{21}\partial^2 p_{L1}/\partial \xi^2$ . As the former is significantly higher than the latter, we can conclude that the dissipation effect due to thermal conduction is considerably large compared with that due to viscosity and liquid compressibility in the present study.

#### G. Numerical example of waveform

Figures 11 and 12 show the numerical results. The initial shock waveform is

$$\Delta P^*(x^*, 0) = p_L^* - p_{L0}^* = \begin{cases} 0.2 & (x^* \leq 1.0) \\ 0 & (x^* > 1.0), \end{cases} \quad (104)$$

where  $\Delta P^*(x^*, 0)$  [bar] is the dimensional pressure perturbation in all the cases.

In the micrometer-bubble cases (Figs. 11 and 12), the waveforms quickly disappear (about 0.005 ms), and the dispersion effect causing wave oscillations do not appear due to the large dissipation effect, regardless of the dilute or non-dilute bubbly liquid. The damping speed of the waveforms in the dilute case (Fig. 12) is the same as that in the non-dilute case (Fig. 11). On the contrary, in the millimeter-bubble cases (Figs. 13 and 14), the waveforms attenuate relatively slowly, and the wave oscillations caused by the dispersion effect appear due to the relatively small dissipation effect. These wave oscillations are called “relaxation oscillations (ROs)”<sup>55,56</sup>. The frequency of the ROs is higher for the non-dilute bubbly liquid case (Fig. 13) than for the dilute bubbly liquid case (Fig. 14). The waveform amplitudes tend toward zero at about 5 ms and 5.7 ms for the dilute and non-dilute

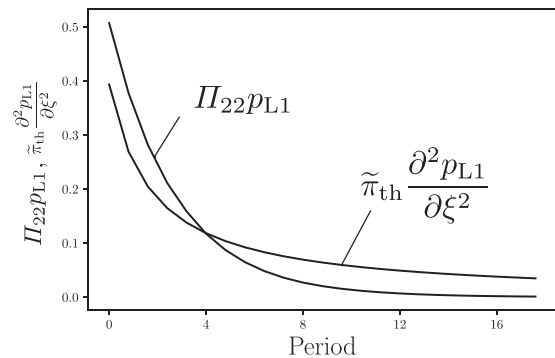
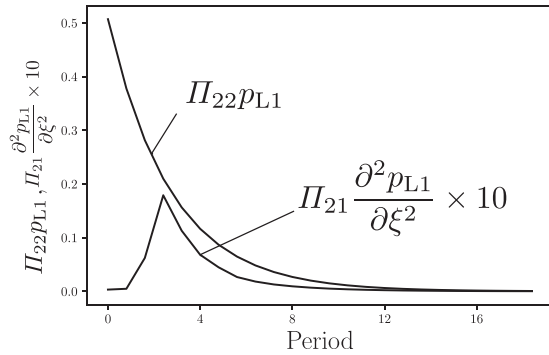


FIG. 9. Numerically obtained temporal evolution of two dissipation terms due to thermal conduction.



**FIG. 10.** Numerically obtained temporal evolution of two dissipation terms in the present study.

bubbly liquid cases, respectively. Thus, the dissipation effect is certainly larger in the dilute bubbly liquid case than that in the non-dilute bubbly liquid case; however, the difference between the two cases is exceedingly small when compared with the dependency of  $R_0^*$ .

The above results show that  $R_0^*$  mainly controlled a degree of the dissipation effect. In this study, we consider the following dissipation factors: (i) viscosity of liquid, (ii) viscosity at the bubble–liquid interface, (iii) liquid compressibility, and (iv) thermal conduction at the bubble–liquid interface. In particular, (ii) and (iv) strongly depend on  $R_0^*$  because the bubble–liquid interface area increases with decreasing  $R_0^*$  under a constant  $\alpha_0$ . In other words, a large dissipation effect for small  $R_0^*$  is caused by the effects of the viscosity and thermal conduction at the bubble–liquid interface.

The small RO frequency in the dilute cases appear to indicate that the medium show a nearly single-phase flow. The number density of bubbles in a bubbly liquid is high when  $\alpha_0$  become small under a constant  $R_0^*$ . Therefore, the dispersion effect is small in the dilute bubbly liquid case due to the small number of bubbles causing the dispersion effect.

## V. CONCLUSIONS

The weakly nonlinear propagation of pressure waves in initially quiescent compressible liquids uniformly containing many spherical microbubbles was theoretically studied by deriving the KdVB equation (73). In particular, the energy equation at the bubble–liquid interface (11) and the effective polytropic exponent (23)<sup>13</sup> were introduced. The main results are summarized as follows:

- (i) The effective polytropic exponent  $\gamma_e$  describing thermodynamics inside the bubble moved closer to unity (i.e., isothermal process) for a small initial bubble radius and to  $\kappa$  (i.e., adiabatic process) for a large initial bubble radius. By introducing the effective polytropic exponent, the form of phase velocity in this study in (56) was altered from that in our previous study.<sup>18</sup>
- (ii) In the present KdVB equation (73), all the coefficients depended on the initial bubble radius,  $R_0^*$ . Although the dissipation coefficient due to the viscosity and liquid compressibility in (77) depended on the initial void fraction  $\alpha_0$ , the other coefficients [i.e., the nonlinear coefficient (75), dissipation coefficient due to thermal conduction (78), and dispersion coefficient (79)] did not depend on  $\alpha_0$ .
- (iii) In the present KdVB equation (73), two types of dissipation terms appeared; one was the well-known second-order derivative term with respect to the space, with the

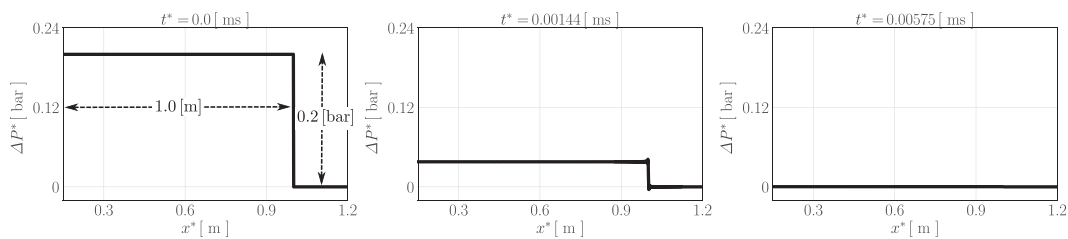


**FIG. 11.** Evolution of initial shock waveform (104) by KdVB equation (73) for non-dilute bubbly liquid and micrometer-bubble case:  $\alpha_0 = 0.01$  and  $R_0^* = 10 \mu\text{m}$ .

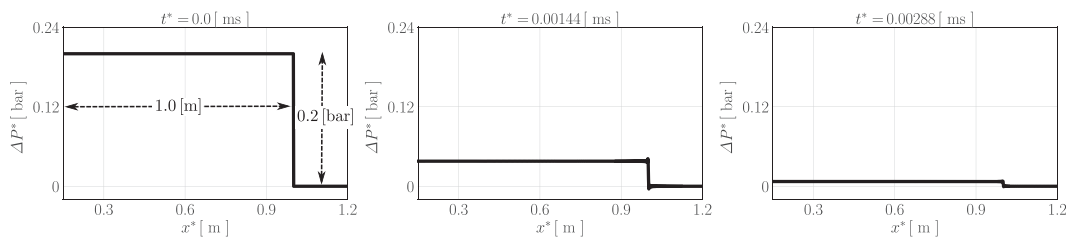


**FIG. 12.** Evolution of initial shock waveform (104) by KdVB equation (73) for dilute bubbly liquid and micrometer-bubble case:  $\alpha_0 = 0.001$  and  $R_0^* = 10 \mu\text{m}$ .

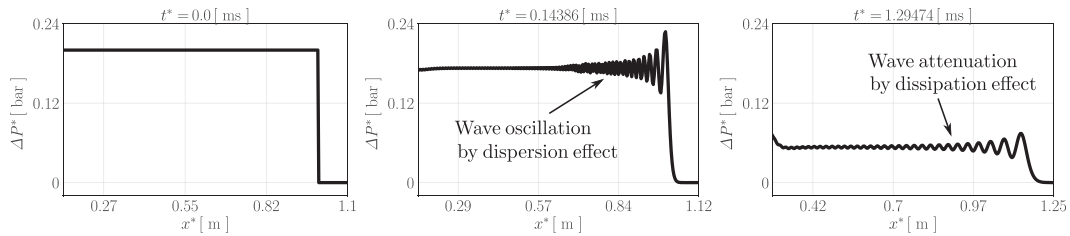


FIG. 13. Evolution of initial shock waveform (104) by KdVB equation (73) for non-dilute bubbly liquid and millimeter-bubble case:  $\alpha_0 = 0.01$  and  $R_0^* = 1$  mm.

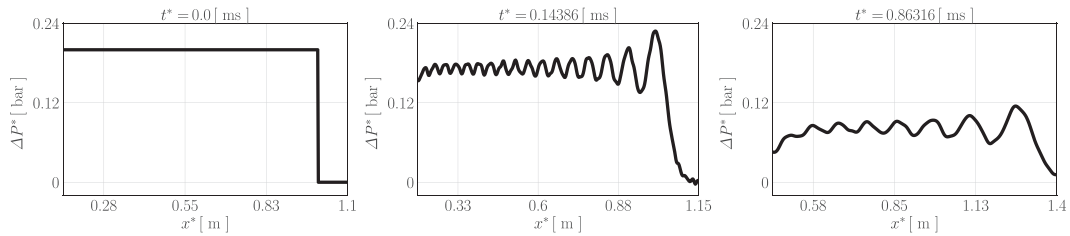


FIG. 14. Evolution of initial shock waveform (104) by KdVB equation (73) for dilute bubbly liquid and millimeter-bubble case:  $\alpha_0 = 0.001$  and  $R_0^* = 1$  mm.

coefficient  $\Pi_{21}$  in (77), and the other was the newly discovered term without differentiation, with the coefficient  $\Pi_{22}$  in (78). Viscosity and liquid compressibility (i.e., acoustic radiation) were contained in  $\Pi_{21}$ , and thermal conductivity was in  $\Pi_{22}$ .

- (iv) The thermal effect in the present study contributed not only to the dissipation coefficients  $\Pi_{21}$  and  $\Pi_{22}$  but also to the nonlinear coefficient  $\Pi_1$  in (75).
- (v) According to (iv), the nonlinearity (i.e., absolute value of the nonlinear coefficient) in this study increased compared with that in our previous study<sup>18</sup> and Prosperetti.<sup>13</sup> In particular, the present nonlinear coefficient  $\Pi_1$  was affected due to the introduction of energy equation (11). Furthermore, the consideration of the thermal effect increased the nonlinearity in bubble oscillations [i.e., Keller equation (12)]; moreover, the nonlinear coefficient in this study increased compared with that in our previous study.<sup>18</sup>
- (vi) In this study, four temperature-gradient models, (18)–(21)<sup>48–51</sup> were utilized to evaluate the thermal dissipation effect. A significant difference among the four models was observed for the microscale bubbles but not for the millimeter-scale bubbles.
- (vii) The thermal dissipation term in this study was a term without differentiation,  $\Pi_{22}f$ , while that in the work of Prosperetti<sup>13</sup> was the second-order derivative with respect to the space,  $\widehat{\pi}_{th} \partial^2 f / \partial \xi^2$ . Numerical analysis revealed that the order of  $\Pi_{22}f$  was comparable with that of  $\widehat{\pi}_{th} \partial^2 f / \partial \xi^2$  although the mathematical forms differed.
- (viii) Further, numerical analysis also revealed that the order of the dissipation term due to thermal conduction,  $\Pi_{22}f$ , was higher than that due to viscosity and acoustic radiation,  $\Pi_{21} \partial^2 f / \partial \xi^2$ .

The above results provide an exhaustive understanding regarding the influence of the thermal effect inside bubbles on the pressure wave in bubbly liquids using the framework of weakly nonlinear theory (i.e., KdVB equation). In our forthcoming study, we will introduce the temperature in the liquid phase as an unknown variable, incorporate the effect of mass transfer across the bubble–liquid interface and the shell surrounding gas bubbles.

## ACKNOWLEDGMENTS

This work was partially carried out with the aid of the JSPS KAKENHI (Grant No. 18K03942) and the Casio Science Promotion Foundation. We would like to thank the referees for their valuable comments and Editage ([www.editage.com](http://www.editage.com)) for English language editing.

## APPENDIX: NUMERICAL SCHEME FOR (72)

The split-step method<sup>57</sup> is used to calculate the KdVB equation containing an advection term with the variable coefficient (73). Equation (73) is divided into two equations, i.e., the linear equation (A1) and the nonlinear equation (A2),

$$\frac{\partial f}{\partial \tau} = -\Pi_{21} \frac{\partial^2 f}{\partial \xi^2} - \Pi_{22} f - \Pi_3 \frac{\partial^3 f}{\partial \xi^3}, \quad (\text{A1})$$

$$\frac{\partial f}{\partial \tau} = -\frac{\Pi_1}{2} \frac{\partial f^2}{\partial \xi}. \quad (\text{A2})$$

First, (A1) is calculated using the spectral method, and the dependent variables  $f^{\text{linear}}(\xi, \tau + \Delta\tau)$  are then obtained. Next, (A2) is calculated using the spectral method and the fourth-order

Runge–Kutta method for temporal marching with  $f^{\text{linear}}$  as the initial condition, and the dependent variables  $f(\xi, \tau + \Delta\tau)$  are thereby obtained. The periodic boundary condition is used.

## DATA AVAILABILITY

The data that support the findings of this study are available from the corresponding author upon reasonable request.

## REFERENCES

- <sup>1</sup>G. B. Whitham, *Linear and Nonlinear Waves* (Wiley, New York, 1974).
- <sup>2</sup>L. van Wijngaarden, “On the equations of motion for mixtures of liquid and gas bubbles,” *J. Fluid Mech.* **33**, 465–474 (1968).
- <sup>3</sup>S. M. Frolov, K. A. Avdeev, V. S. Aksenov, A. A. Borisov, F. S. Frolov, I. O. Shamshin, R. R. Tikhvatullina, B. Basara, W. Edelbauer, and K. Pachler, “Experimental and computational studies of shock wave-to-bubbly water momentum transfer,” *Int. J. Multiphase Flow* **92**, 20–38 (2017).
- <sup>4</sup>Y. Zhang, Z. Guo, Y. Gao, and X. Du, “Acoustic wave propagation in bubbly flow with gas, vapor or their mixtures,” *Ultrason. Sonochem.* **40**, 40–45 (2018).
- <sup>5</sup>M. A. Maiga, O. Coutier-Delgosha, and D. Buisine, “A new cavitation model based on bubble-bubble interactions,” *Phys. Fluids* **30**, 123301 (2018).
- <sup>6</sup>R. Oguri and K. Ando, “Cavitation bubble nucleation induced by shock-bubble interaction in a gelatin gel,” *Phys. Fluids* **30**, 051904 (2018).
- <sup>7</sup>H. Zhang, Z. Zuo, K. A. Mørch, and S. Liu, “Thermodynamic effects on Venturi cavitation characteristics,” *Phys. Fluids* **31**, 097107 (2019).
- <sup>8</sup>R. R. Tikhvatullina and S. M. Frolov, “Numerical simulation of shock and detonation waves in bubbly liquids,” *Shock Waves* **30**, 263–271 (2020).
- <sup>9</sup>M. Brunhart, C. Soteriou, M. Gavaises, I. Karathanassis, P. Koukouvinis, S. Jahangir, and C. Poelma, “Investigation of cavitation and vapor shedding mechanisms in a Venturi nozzle,” *Phys. Fluids* **32**, 083306 (2020).
- <sup>10</sup>A. Jeffrey and T. Kawahara, *Asymptotic Methods in Nonlinear Wave Theory* (Pitman, London, 1982).
- <sup>11</sup>L. van Wijngaarden, “One-dimensional flow of liquids containing small gas bubbles,” *Annu. Rev. Fluid Mech.* **4**, 369–396 (1972).
- <sup>12</sup>L. Noordzij and L. van Wijngaarden, “Relaxation effects, caused by relative motion, on shock waves in gas-bubble/liquid mixtures,” *J. Fluid Mech.* **66**, 115–143 (1974).
- <sup>13</sup>A. Prosperetti, “The thermal behaviour of oscillating gas bubbles,” *J. Fluid Mech.* **222**, 587–616 (1991).
- <sup>14</sup>R. I. Nigmatulin, *Dynamics of Multiphase Media, Part 2* (Hemisphere, New York, 1991).
- <sup>15</sup>N. A. Gumerov, “Quasi-monochromatic weakly non-linear waves in a low-dispersion bubble medium,” *J. Appl. Math. Mech.* **56**, 50–59 (1992).
- <sup>16</sup>D. B. Khismatullin and I. S. Akhatov, “Sound-ultrasound interaction in bubbly fluids: Theory and possible applications,” *Phys. Fluids* **13**, 3582–3598 (2001).
- <sup>17</sup>T. Kanagawa, T. Yano, M. Watanabe, and S. Fujikawa, “Unified theory based on parameter scaling for derivation of nonlinear wave equations in bubbly liquids,” *J. Fluid Sci. Technol.* **5**, 351–369 (2010).
- <sup>18</sup>T. Kanagawa, M. Watanabe, T. Yano, and S. Fujikawa, “Nonlinear wave equations for pressure wave propagation in liquids containing gas bubbles (comparison between two-fluid model and mixture model),” *J. Fluid Sci. Technol.* **6**, 838–850 (2011).
- <sup>19</sup>N. A. Kudryashov and D. I. Sinelshchikov, “An extended equation for the description of nonlinear waves in a liquid with gas bubbles,” *Wave Motion* **50**, 351–362 (2013).
- <sup>20</sup>N. A. Kudryashov and D. I. Sinelshchikov, “Extended models of nonlinear waves in liquid with gas bubbles,” *Int. J. Nonlinear Mech.* **63**, 31–38 (2014).
- <sup>21</sup>T. Kanagawa, “Two types of nonlinear wave equations for diffractive beams in bubbly liquids with nonuniform bubble number density,” *J. Acoust. Soc. Am.* **137**, 2642–2654 (2015).
- <sup>22</sup>J. M. Tu, S. F. Tian, M. J. Xu, X. Q. Song, and T. T. Zhang, “Bäcklund transformation, infinite conservation laws and periodic wave solutions of a generalized (3+1)-dimensional nonlinear wave in liquid with gas bubbles,” *Nonlinear Dyn.* **83**, 1199–1215 (2016).
- <sup>23</sup>P. M. Jordan, “A survey of weakly-nonlinear acoustic models: 1910–2009,” *Mech. Res. Commun.* **73**, 127–139 (2016).
- <sup>24</sup>R. J. Thiessen and A. F. Cheviakov, “Nonlinear dynamics of a viscous bubbly fluid,” *Commun. Nonlinear Sci. Numer. Simul.* **73**, 244–264 (2019).
- <sup>25</sup>T. Maeda and T. Kanagawa, “Derivation of weakly nonlinear wave equations for pressure waves in bubbly flows with different types of nonuniform distribution of initial flow velocities of gas and liquid phases,” *J. Phys. Soc. Jpn.* **89**, 114403 (2020).
- <sup>26</sup>T. Yatabe, T. Kanagawa, and T. Ayukai, “Theoretical elucidation of effect of drag force and translation of bubble on weakly nonlinear pressure waves in bubbly flows,” *Phys. Fluids* **33**, 033315 (2021).
- <sup>27</sup>T. Kanagawa, T. Ayukai, T. Kawame, and R. Ishitsuka, “Weakly nonlinear theory on pressure waves in bubbly liquids with a weak polydispersity,” *Int. J. Multiphase Flow*, in press (2021).
- <sup>28</sup>V. V. Kuznetsov, V. E. Nakoryakov, B. G. Pokusaev, and I. R. Shreiber, “Propagation of perturbations in a gas-liquid mixture,” *J. Fluid Mech.* **85**, 85–96 (1978).
- <sup>29</sup>D. S. Drumheller, M. E. Kipp, and A. Bedford, “Transient wave propagation in bubbly liquids,” *J. Fluid Mech.* **119**, 347–365 (1982).
- <sup>30</sup>A. E. Beylich and A. Gülhan, “On the structure of nonlinear waves in liquids with gas bubbles,” *Phys. Fluids A* **2**, 1412–1428 (1990).
- <sup>31</sup>T. Kamei and T. Kanagawa, “Two types of nonlinear pressure waves in bubbly liquids incorporating viscosity and thermal conductivity,” in *ASME Proceedings of Series 5 AJKFluids2019-4663* (2019).
- <sup>32</sup>T. Kamei, T. Ayukai, and T. Kanagawa, “Theoretical study on an effect of liquid viscosity and thermal conductivity on weakly nonlinear propagation of long pressure waves in bubbly liquids,” *J. JSCE, Ser. A2* **75**, 499–508 (2019).
- <sup>33</sup>D. Fuster and F. Montel, “Mass transfer effects on linear wave propagation in diluted bubbly liquids,” *J. Fluid Mech.* **779**, 598–621 (2015).
- <sup>34</sup>C. C. Church, “The effects of an elastic solid surface layer on the radial pulsations of gas bubbles,” *J. Acoust. Soc. Am.* **97**, 1510–1521 (1995).
- <sup>35</sup>L. Hoff, P. C. Sontum, and J. M. Hovem, “Oscillations of polymeric microbubbles: Effect of the encapsulating shell,” *J. Acoust. Soc. Am.* **107**, 2272–2280 (2000).
- <sup>36</sup>M. Versluis, E. Stride, G. Lajoinie, B. Dollet, and T. Segers, “Ultrasound contrast agent modeling: A review,” *Ultrasound Med. Biol.* **46**, 2117–2144 (2020).
- <sup>37</sup>Y. Kikuchi and T. Kanagawa, “Weakly nonlinear theory on ultrasound propagation in liquids containing many microbubbles encapsulated by visco-elastic shell,” *Jpn. J. Appl. Phys.* **60**, in press (2021).
- <sup>38</sup>M. Ishii, “One-dimensional drift-flux model and constitutive equations for relative motion between phases in various two-phase flow regimes,” *ANL Report No. ANL-77-47*, 1977.
- <sup>39</sup>I. Kataoka, “Modelling and basic equations of gas-liquid two-phase flow,” *Jpn. J. Multiphase Flow* **5**, 3–21 (1991).
- <sup>40</sup>I. Akhatov, U. Parlitz, and W. Lauterborn, “Towards a theory of self-organization phenomena in bubble-liquid mixtures,” *Phys. Rev. E* **54**, 4990–5003 (1996).
- <sup>41</sup>R. Egashira, T. Yano, and S. Fujikawa, “Linear wave propagation of fast and slow modes in mixtures of liquid and gas bubbles,” *Fluid Dyn. Res.* **34**, 317–334 (2004).
- <sup>42</sup>T. Yano, T. Kanagawa, M. Watanabe, and S. Fujikawa, “Nonlinear wave propagation in bubbly liquids,” in *Shock Wave Science and Technology Reference Library* (Springer, 2013).
- <sup>43</sup>G. I. Taylor, “The viscosity of a fluid containing small drops of another fluid,” *Proc. R. Soc. London, Ser. A* **138**, 41–48 (1932).
- <sup>44</sup>W. R. Schowalter, C. E. Chaffey, and H. Brenner, “Rheological behavior of a dilute emulsion,” *J. Colloid Interface Sci.* **26**, 152–160 (1968).
- <sup>45</sup>S. J. Choi and W. R. Schowalter, “Rheological properties of nondilute suspensions of deformable particles,” *Phys. Fluids* **18**, 420–427 (1975).
- <sup>46</sup>A. Einstein, “Eine neue bestimmung der Moleküldimensionen,” *Ann. Phys.* **19**, 289–306 (1906).
- <sup>47</sup>Y. Murai, T. Shiratori, I. Kumagai, P. A. Rühs, and P. Fischer, “Effective viscosity measurement of interfacial bubble and particle layers at high volume fraction,” *Flow Meas. Instrum.* **41**, 121–128 (2015).
- <sup>48</sup>R. E. Caflisch, M. J. Miksis, G. C. Papanicolaou, and L. Ting, “Effective equations for wave propagation in bubbly liquids,” *J. Fluid Mech.* **153**, 259–273 (1985).
- <sup>49</sup>G. Zhou and A. Prosperetti, “Modelling the thermal behaviour of gas bubbles,” *J. Fluid Mech.* **901**, R3 (2020).

- <sup>50</sup>J. B. Keller and I. I. Kolodner, "Damping of underwater explosion bubble oscillations," *J. Appl. Phys.* **27**, 1152–1161 (1956).
- <sup>51</sup>M. Shimada, Y. Matsumoto, and T. Kobayashi, "Dynamics of the cloud cavitation and cavitation erosion," *Trans. JSME, Ser. B* **65**, 1934–1940 (1999).
- <sup>52</sup>B. Lertnuwat, K. Sugiyama, and Y. Matsumoto, "Modelling of thermal behavior inside a bubble," in Proceedings of 4th International Symposium on Cavitation, B6.002 (2001).
- <sup>53</sup>A. Preston, T. Colonius, and C. E. Brennen, "A reduced-order model of heat transfer effects on the dynamics of bubbles," in Proceedings of ASME FEDSM'02, FEDSM2002-31026(CD-ROM) (2002).
- <sup>54</sup>K. Sugiyama, S. Takagi, and Y. Matsumoto, "A new reduced-order model for the thermal damping effect on radial motion of a bubble (1st report, perturbation analysis)," *Trans. JSME, Ser. B* **71**, 1011–1019 (2005).
- <sup>55</sup>M. Kameda, N. Shimauro, F. Higashino, and Y. Matsumoto, "Shock waves in a uniform bubbly flow," *Phys. Fluids* **10**, 2661–2668 (1998).
- <sup>56</sup>K. Ando, T. Colonius, and C. E. Brennen, "Numerical simulation of shock propagation in a polydisperse bubbly liquid," *Int. J. Multiphase Flow* **37**, 596–608 (2011).
- <sup>57</sup>G. M. Musulu and H. A. Erbay, "A split-step Fourier method for the complex modified Korteweg–de Vries equation," *Comput. Math. Appl.* **45**, 503–514 (2003).